- Ellipticals satisfy their own rotation-luminosity correlation, $L \propto \sigma_0^4$ which is known as the **Faber-Jackson relation**. Originating in 1976, it actually pre-dates the first specification of the Tully-Fisher relation. Herein, σ_0 is the velocity dispersion averaged over the galaxy.

Plot: Faber-Jackson Relation for Ellipticals

∗ It is again a consequence of flat rotation curves, fixed mass-to-light ratios and surface brightnesses, though slightly more virialized than for spirals.

∗ There is considerable scatter, with a significant contribution from the large range of masses and sizes in the variety of ellipticals.

- The scatter can be substantially reduced by exploring a key third dimension, the effective radius r_e of elliptical profiles. This can be obtained via isophote determination in imaging. The result is a tighter correlation that is a result of a coupling between r_e and the velocity dispersion σ :

$$\boxed{L \;\propto\; \sigma_0^{2.65}\, r_e^{0.65} \quad .} \tag{18}$$

This almost defines a surface in the 3D space of $(L,\, \sigma_0,\, r_e)$, and this is known as the **fundamental plane** for ellipticals.

Plot: Parametric Views of the Fundamental Plane for Ellipticals

Faber-Jackson Relation for Ellipticals

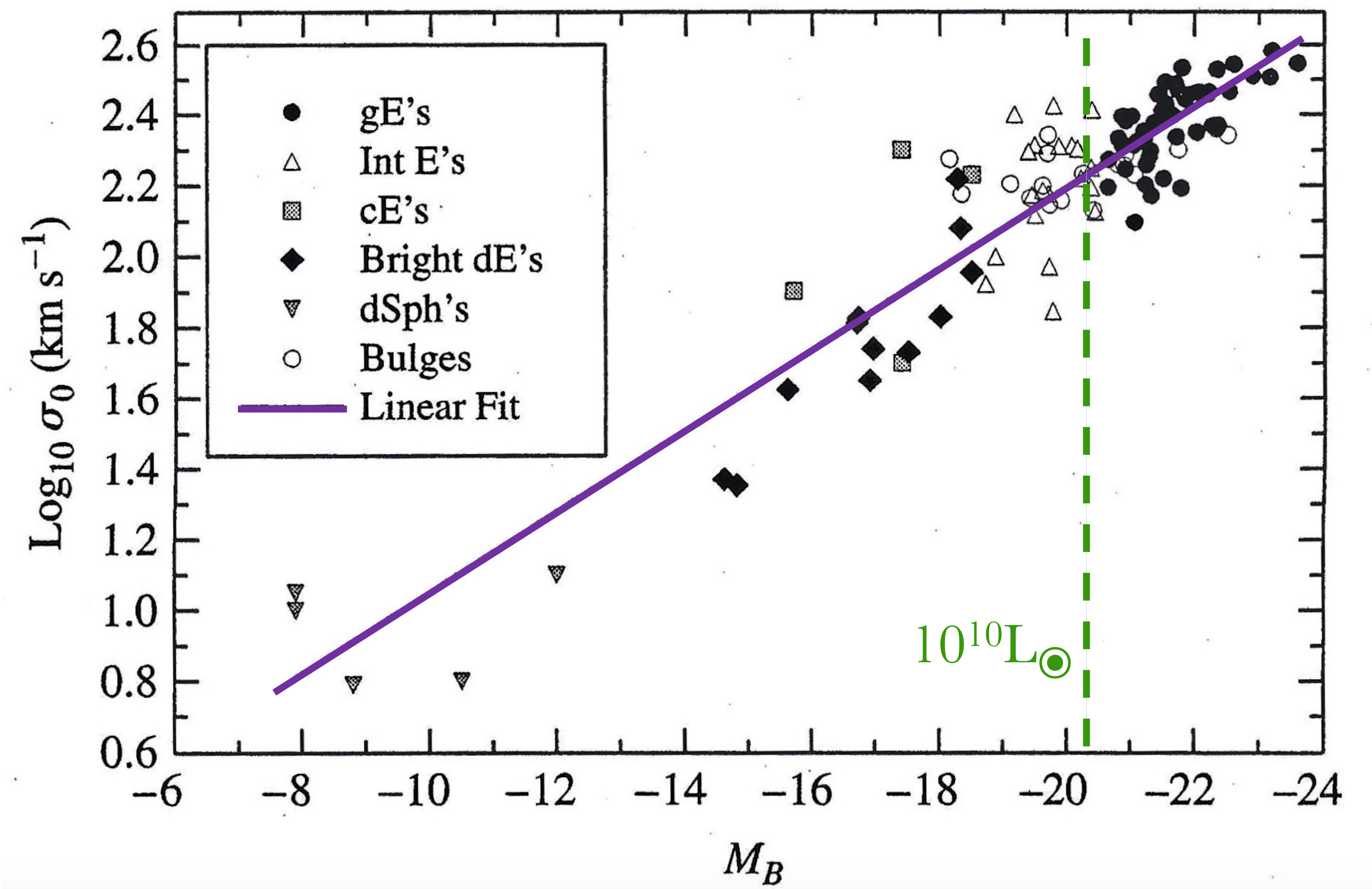

- Faber-Jackson relation: circular velocity v_c versus absolute magnitude for elliptical galaxies. Figure 25.33 from Carroll+Ostlie; data from Bender et al., ApJ **399**, 462, (1992).

Fundamental Plane for Ellipticals

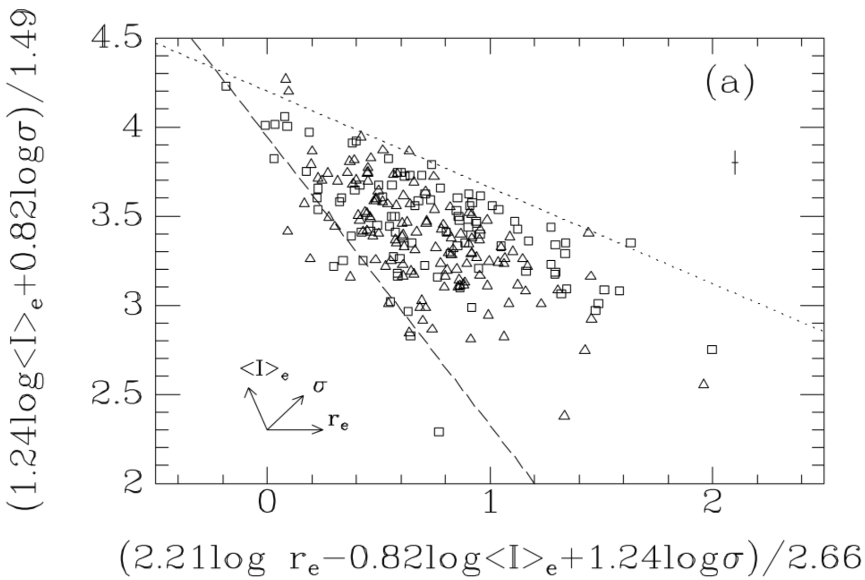

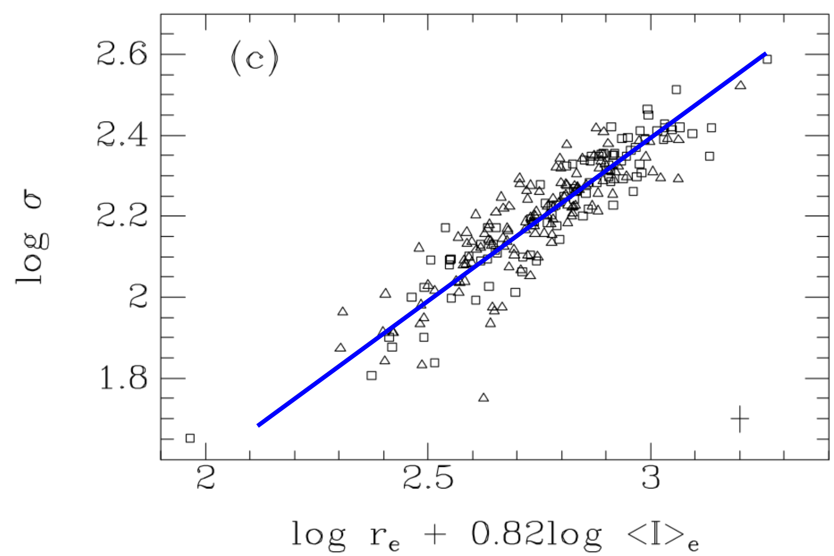

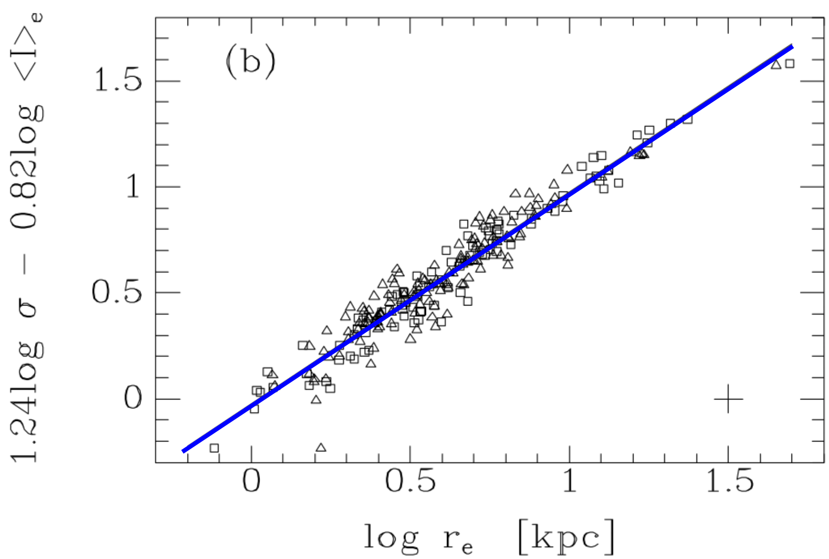

- (a) The ($<I>, \sigma, r_e$) plane viewed face-on, illustrating the substantial scatter.
- (b) and (c): two edge-on views of the fundamental plane, demonstrating reduced (but non-zero) scatter.
- Jorgensen et al. MNRAS **280**, 167 (1996)

5.2 King's Model: Spherical Galaxies

• As a simple models of ellipticals, let us consider spherical potentials (pertinent to E0s), and so eliminate the role of angular momentum. In general, the kinetic distribution function of stars takes the form $f(E, \vec{J})$, so that we shall set $|\vec{J}| \to 0$. Then

Combes, et al. Ch. 4

$$f(E, \vec{J}) \;\to\; f(E) \;=\; \frac{\rho_0}{(2\pi\sigma^2)^{3/2}} \,\exp\left\{-\frac{E}{\sigma^2}\right\} \quad . \tag{19}$$

Here σ^2 is the velocity dispersion. Hence, $E \equiv v^2/2 + \Phi(r)$ is the *energy per unit mass*, with $\Phi(r)$ being a spherical gravitational potential.

∗ Most such spherical models invoke this **isotropic, isothermal sphere** assumption: σ^2 is independent of r. Here $f(E)$ resembles a Maxwellian, yet is a function of energy per unit mass E, not energy per particle. The isotropy then establishes the velocity dispersions (in spherical polar coordinates):

$$\langle v_r^2 \rangle \;=\; \frac{1}{\rho_0} \int v_r^2 \, f\left(\frac{1}{2} \sum_i v_i^2 + \Phi \right) dv_r \, dv_\theta \, dv_\phi \;\equiv\; \langle v_\theta^2 \rangle \;\equiv\; \langle v_\phi^2 \rangle \tag{20}$$

• Integrating Eq. (19) over d^3v gives the stellar density profile in the galaxy (or globular cluster):

$$\rho(r) \;\equiv\; \int f \, d^3v \;=\; \rho_0 \,\exp\left\{-\frac{\Phi(r)}{\sigma^2}\right\} \quad . \tag{21}$$

The field induced by this density is derived by Poisson's equation:

$$\nabla^2\Phi \;=\; 4\pi G\rho(r) \quad \Rightarrow \quad \frac{1}{r^2}\frac{\partial}{\partial r}\left(r^2 \frac{\partial\Phi}{\partial r} \right) \;=\; 4\pi G\rho_0 \,\exp\left\{-\frac{\Phi(r)}{\sigma^2}\right\} \quad , \tag{22}$$

using the spherical polar coordinate form of the Laplacian operator. While this ODE, in general, requires numerical solution, it is simply shown (by taking derivatives; constants of integration can be absorbed in the definition of r_c) that asymptotically an approximate solution is

$$\Phi(r) \;\approx\; 2\sigma^2 \log_e\left(\frac{r}{r_c} \right) \quad , \quad r_c \;=\; \frac{3\sigma}{\sqrt{4\pi G\rho_0}} \quad . \tag{23}$$

This generates an $\rho \propto 1/r^2$ density profile, valid for $r \lesssim r_c$, where $\Phi(r) < 0$.

• A more realistic variation of the distribution in Eq. (19) incorporates a truncation that models the escape of stars from a galaxy near infinity:

$$f(E) \;=\; \begin{cases} 0 \quad , & E \geq E_0 \quad , \\ \dfrac{\rho_0}{(2\pi\sigma^2)^{3/2}} \left\{ \exp\left(-\dfrac{(E-E_0)}{\sigma^2} \right\} - 1 \right\} \quad , & E < E_0 \quad , \end{cases} \tag{24}$$

where $E_0 < 0$ is some binding energy. This distribution function [*sketch it*] defines the **King model**. Integration over v gives

$$\frac{\rho(r)}{\rho_0} \;=\; e^y \,\mathrm{erf}\Bigl(\sqrt{y}\Bigr) - \sqrt{\frac{4y}{\pi}} \left(1 + \frac{2y}{3} \right) \quad , \quad y \;=\; \frac{E_0 - \Phi(r)}{\sigma^2} \quad , \tag{25}$$

Here

$$\mathrm{erf}(x) \;=\; \frac{2}{\sqrt{\pi}} \int_0^x e^{-u^2}\, du \tag{26}$$

is the error function, of fame in probability theory. This $\rho(r)$ is inserted into Poisson's equation to solve for $\Phi(r)$ and then $\rho(r)$ numerically.

Plot: Comparison of King Model with $r^{1/4}$ Empirical Model

∗ At large r, there must exist a **tidal radius** r_t at which $y = 0$ and $\rho(r_t) = 0$ so that $M = M(r_t)$ is the total mass of the system. Then $E_0 = -GM/r_t$ is the effective binding energy.

• ρ_0 and the **core radius** r_c are two scale factors and r_t is a parameter for the King model. Often, we use the **concentration parameter** $c = \log_e(r_t/r_c)$ instead. For ellipticals, $c \approx 2.2$, while for globular clusters $c \approx 1$. Hence, tidal interactions are much more important for GCs.

Plot: King model profiles

• The differences in density concentrations for these two self-gravitating systems in part reflects their comparitive gravitational relaxation timescales, as discussed in Section 6.1 below.

King Model for Elliptical NGC 3379

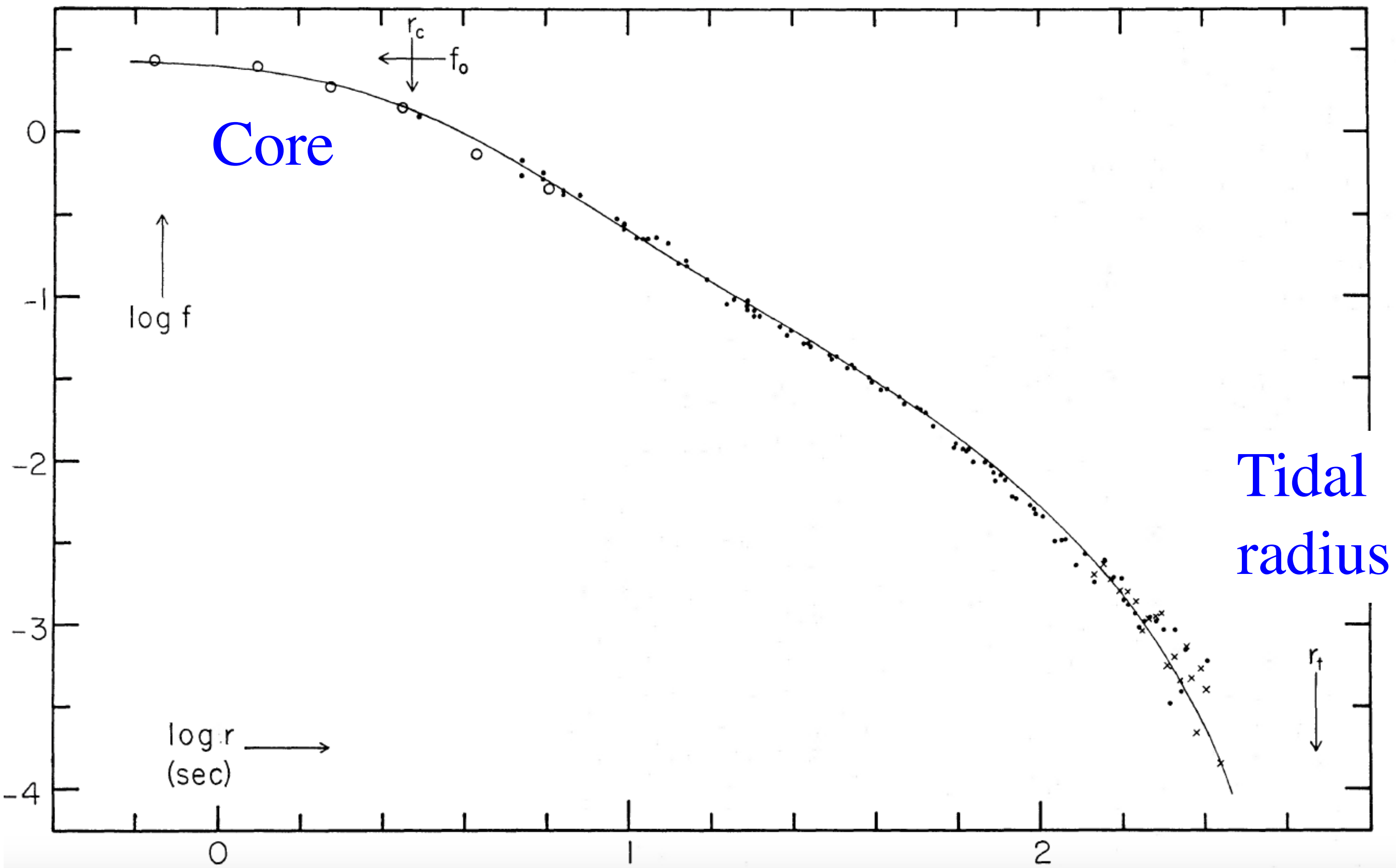

- King model of concentration c=2.2 for NGC 3379. Circles, crosses and squares represent data taken using different techniques in different optical wavebands suited to the measurement. King, AJ 71, 64 (1966)

King Model Profiles

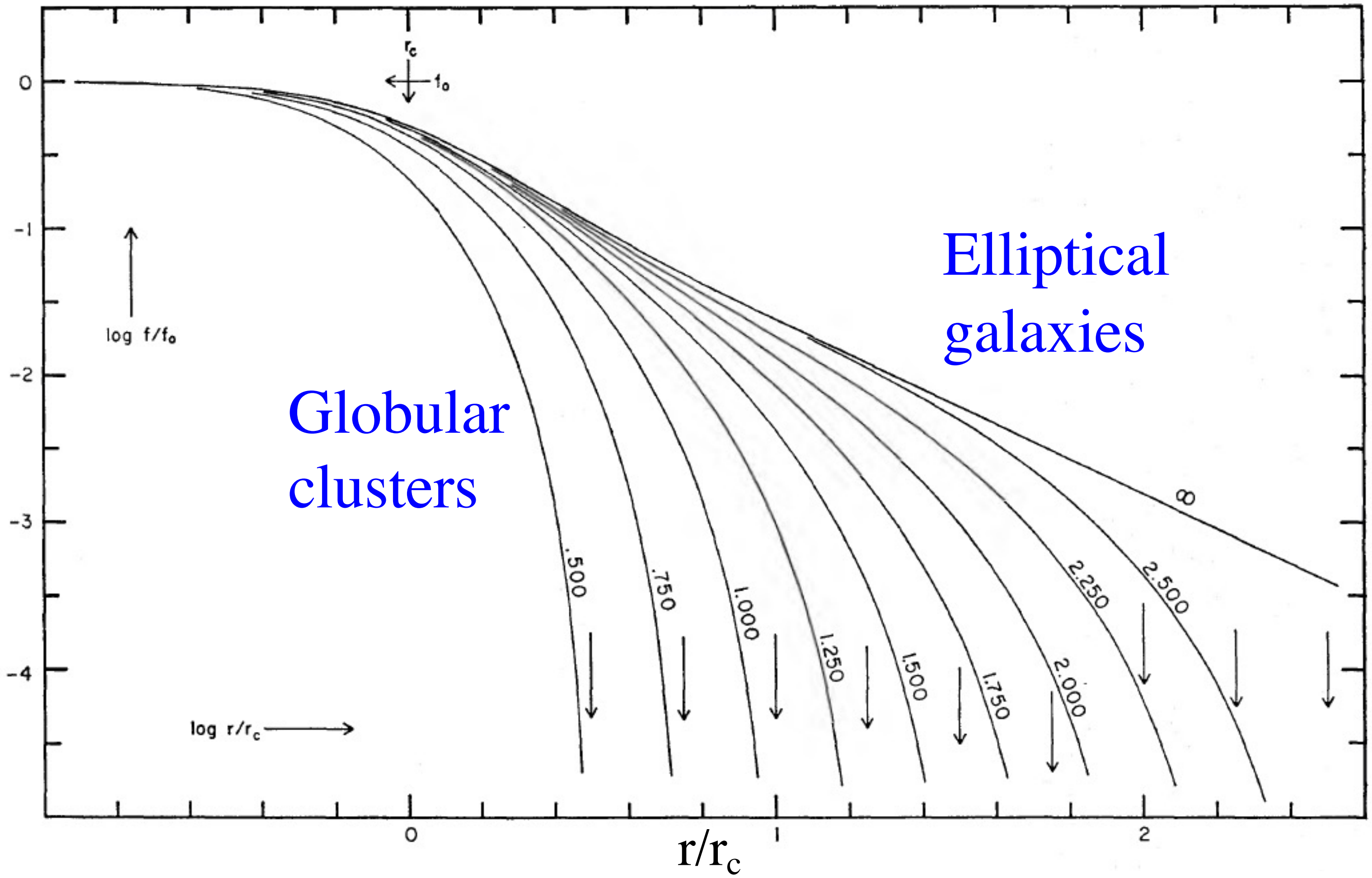

- King (1966, AJ) model profiles for various concentration parameters $c=\log(r_t/r_c)$ as labelled. Globular clusters tend to be more concentrated in their stellar density/light profiles than elliptical galaxies.

6 Galactic Evolution

C & O, Sec. 24.2

To develop a general sense of the dynamical timescale for the formation of elliptical galaxies, we estimate the **collapse timescale** for stellar ensembles. We will assume that pressure gradients don't influence the infall (i.e. $|dP/dr| \ll GM_c\rho_c/r_c^2$), and that the pressure remains nearly constant, so that the collapse is *isothermal*. Newton's law for this gravitating system is

$$\frac{d^2r}{dt^2} = -\frac{GM}{r^2} \quad , \tag{27}$$

cancelling out mass/density factors and letting r denote the time-dependent radius of the stellar cloud, initially r_c.

Since mass shells do not cross during homologous collapse in this simplified scenario, the enclosed mass is a constant of the motion, so we can set $M = M_c = 4\pi\rho_c r_c^3/3$. Multiplying by dr/dt leads to a perfect derivative, so that the ODE integrates to

$$\frac{dr}{dt}\cdot\frac{d^2r}{dt^2} = -\frac{GM}{r^2}\cdot\frac{dr}{dt} \quad \Rightarrow \quad \frac{1}{2}\left(\frac{dr}{dt}\right)^2 = \frac{4\pi}{3}\,G\rho_c r_c^3\left(\frac{1}{r}-\frac{1}{r_c}\right) \quad . \tag{28}$$

Here we set $dr/dt = 0$ initially, i.e. at $r = r_c$. Then setting $\theta = r/r_c$, we solve

$$\frac{d\theta}{dt} = -\frac{\pi}{2t_{\rm ff}}\sqrt{\frac{1}{\theta}-1} \quad \text{for} \quad t_{\rm ff} = \sqrt{\frac{3\pi}{32}\,\frac{1}{G\rho_c}} \quad , \tag{29}$$

using the substitution $\theta = \cos^2\zeta$. The result is

$$\zeta + \frac{1}{2}\sin 2\zeta = \frac{\pi t}{2t_{\rm ff}} \quad . \tag{30}$$

This cycloidal solution has an analogy of bouncing closed universes in a closed Newtonian cosmology.

• Since initially $\zeta = 0$ corresponding to $\theta = 1$, the radius of the sphere reaches zero when $\zeta = \pi/2$, so that $t_{\rm ff}$ is the **free-fall timescale**. This could be established using dimensional analysis only under isothermal assumptions.

∗ Assuming $\rho_0 = 3M/(4\pi R^3) = 8\times 10^{-26}\,\text{g cm}^{-3}$, this leads to an estimate of $t_{\rm ff} \sim 200\,\text{Myr}$; i.e. much shorter than the age of galaxies.

• This motivates the Eggen Lynden-Bell and Sandage (1962) collapse model (EGS model), which focuses primarily (but not exclusively) on spiral galaxies, for which the free-fall description is applied to the proto-galactic gas cloud.

∗ The structure of the cloud essentially bifurcates, with a component that has older, high-velocity stars in elliptical orbits that sample high latitudes. These persist in their motions at large radii, and form the precursor of halos with globular clusters. The angular momentum of this component is small, and so it remains buoyant and ellipsoidal.

∗ The inner component has much more gas, and higher angular momentum. It is prone to the gravitational free-fall just described and so condenses. The angular momentum halts collapse earlier in the plane of rotation, through the influences of centrifugal forces, and this leads to disk formation. The higher densities yield greater radiative dissipation and promote stellar evolution, leading to a higher metallicity environment in and near the disk.

Plot: Milky Way Structural Schematic - Revisited

6.1 Gravitational Relaxation

• Formation of spiral galaxy halos, ellipticals and globular clusters is similar in several ways, most notably due to the profound absence of gas. Therefore the free-fall description is not the most accurate, particularly later on during the evolution when the system becomes much denser. The proto-galactic relaxation can be effected through gravitational stellar collisions, which provides an **effective thermodynamic buoyancy**, we explore here.

Combes, et al. Ch. 4

∗ This relaxation is analogous to the Coulomb problem for ionized gases because of the common inverse square nature of the electrostatic and gravitational force laws. Through energy exchange, it acts to essentially thermalize the stellar velocities.

For a number density n of stars of typical mass M and typical speed v (obtainable via the measured velocity dispersion), the **relaxation time** is

Schematic of the Milky Way

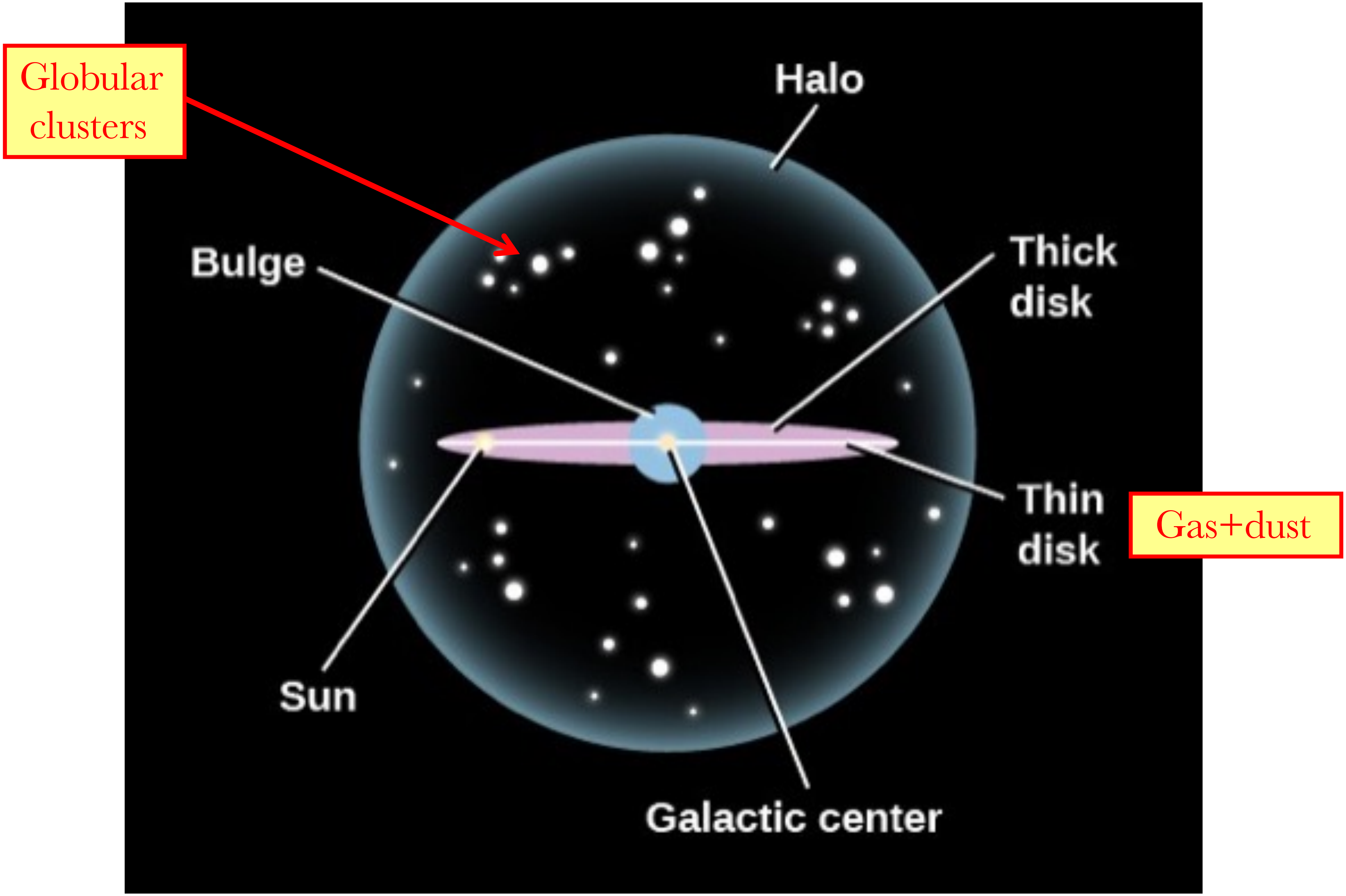

given by

$$t_{\rm rel} \;=\; \frac{v^3}{8\pi n\, G^2 M^2\, \log_e (R/b)} \quad . \tag{31}$$

Here b is called the *impact parameter* for stellar gravitation collisions, effectively the mean separation of stars. Hence, for $\mathcal{N}$ stars in a self-gravitating system, it is given by $(R/b)^3 = \mathcal{N}$. Since $n = 3\mathcal{N}/(4\pi R^3)$ and $v^2 \sim G\mathcal{N}M/R$ defines the virial speed, the relaxation time can be expressed in terms of the ballistic **crossing time** $t_{\rm c} = R/v$ for the volume:

$$\frac{t_{\rm rel}}{t_{\rm c}} \;=\; \frac{v^4}{8\pi n\, G^2 M^2 R\, \log_e (R/b)} \sim \frac{1}{6}\,\frac{\mathcal{N}}{\log_e \mathcal{N}} \quad . \tag{32}$$

• Therefore, the ratio of the relaxation time to the dynamic crossing time *is purely a function of the number of stars in the system.*

∗ Hence, for globular clusters, $\mathcal{N} \sim 10^5$, $t_c \sim 10^6$ years $\Rightarrow t_{\rm rel} \lesssim t_{\rm H}$.

∗ In contrast, for ellipticals, $\mathcal{N} \sim 10^{10}$, $t_c \sim 10^8$ years $\Rightarrow t_{\rm rel} \gg t_{\rm H}$. Accordingly, purely collisional relaxation is not sufficient to condense ellipticals.

• **Punchline:** ellipticals are not fully-relaxed at present, and are still evolving collisionally as self-gravitating systems.

The fuller understanding of collisional interactions of stars and their impact on galaxy evolution and interaction has been facilitated through intensive **N-body simulations**. These are the tool of choice for modeling galaxy interactions and large scale structure formation. More recent vintages have incorporated the complexity of gas influences and dissipation.

∗ Such N-body simulations provide insightful models of the nature of galaxy interactions, such as are observed in fascinating images.

Plot: Antennae Galaxies: NGC 4038 and NGC 4039

Antennae Galaxies: HST Image

NGC 4038
& NGC 4039

- ESA Image Gallery